Phase imaging with rotating illumination

Haiyan Wang (王海燕), Cheng Liu (刘 诚)*, Xingchen Pan (潘兴臣),
Jun Cheng (程 君), and Jianqiang Zhu (朱健强)

Shanghai Institute of Optics and Fine Mechanics, Chinese Academy of Sciences, Shanghai 201800, China
*Corresponding author: cheng.liu@hotmail.co.uk

A modified extended-ptychographical-iterative-engine (ePIE) algorithm is proposed to overcome the disadvantages of ePIE technique and reduce the influence of stage hysteresis or backlash error. The exit wave of a rotatable "screen" illuminated by plane wave is used as the illumination on the specimen, and the complex transmission functions of the rotatable object and specimen can be simultaneously reconstructed. Compared with the standard $x - y$ scanning PIE algorithm, the proposed algorithm can completely avoid the influence of stage hysteresis (or backlash error). The proposed algorithm also has higher convergence speed and better accuracy than the standard PIE algorithm.

OCIS codes: 050.1970, 100.5070, 070.0070, 110.3010.
doi: 10.3788/COL201412.010501.

Given the difficulty in manufacturing high-quality optics in X-ray and electron microscopy, coherent diffraction imaging (CDI) is regarded as a promising technique for retrieving phase information from the recorded diffraction pattern intensity. Considering that CDI directly reconstructs the complex amplitude from the far field diffraction, the resolution of CDI is only limited by the diffraction limitation rather than optics quality. CDI algorithm based on iterative scheme was first suggested by Gerchberg and Saxton[1] and then developed by Fienup[2,3]. The basic principle of CDI algorithm is to repeatedly propagate the light field forward and backward between the object and recording planes while various constraints are used for the field updating; the final result on object plane is regarded as the real distribution of the object function[4]. Aside from the simplicity of experimental setup, CDI method has better performance in imaging speed and noise immunization; numerous researches have used this method in the fields of adaptive optics[5], laser beam quality detection[6], optical encryption[7], diffraction optics, and biological imaging. However, traditional CDI method needs an isolated object. Furthermore, for most specimens, the convergence speed is low and the performance is unreliable. Researches have been conducted to overcome these disadvantages in CDI[8,9]. Rodenburg suggested a new CDI technique named ptycholographical iterative engine (PIE), wherein a set of diffraction patterns are recorded in the far field, and the specimen illuminated by a light beam is scanned in the x- and y-directions. Moreover, a Wigner filter-like formula is used to reconstruct the object iteratively. Compared to traditional CDI techniques, PIE has much faster convergence and higher reliability. At present, PIE has been successfully demonstrated with visible light, X-ray, and electron beam[10−13]. In standard PIE algorithm, the illumination probe must be accurately determined. However, for most experiments, this process is difficult or impossible because the parameters of the optics that form the illumination cannot be accurately determined. Thus, the estimation of the illumination is a huge problem for many PIE applications. Currently, this difficulty has been overcome by the extended-PIE (ePIE) algorithm, which can measure

the illumination and the specimen simultaneously[14]. The ePIE technique needs a substantial amount of data and long data acquisition time. Therefore, ePIE performance highly depends on the stability and accuracy of the translation equipment. Given that most translation stages suffer from the hysteresis or backlash error, when the specimen is scanned to very fine mesh grid positions, the hysteresis or backlash error will accumulate. This process finally leads to serious degradation in the reconstruction quality. Recently, Maiden[15] suggested a method of finding the real probe-specimen position with the minimizing-error scheme. However, the backlash error problem is only partially resolved because the suggested method can only find very small position drifting. Hysteresis or backlash error of the translation stage is still a huge problem for ePIE algorithm application, especially for electron beam and x-ray imaging.

This letter proposes a modified ePIE technology using a rotating illumination to replace the $x - y$ scanning of the specimen, which can be used in complex system such as the high power laser system where $x - y$ scanning is unavailable[16]. A planar beam diffracted by a rotatable object illuminates the specimen studied. In addition, the diffraction patterns are recorded in the far field when the object is rotated to angles of $\Delta\theta, 2\Delta\theta, 3\Delta\theta, \cdots m\Delta\theta$. The influence of the hysteresis or backlash error can be reduced completely because the object is always rotated in one given direction. In addition, given that all rotating probes illuminate on the same specimen area, image reconstruction can be observed with a small number of diffraction patterns. Moreover, the data acquisition time and the device stability requirement are reduced.

The principle of the proposed method is schematically shown in Fig. 1, where a screen with transmission function of $T(x_0, y_0)$ is fixed on a rotatable stage. In addition, the exit wave of the screen is used as the illumination on the specimen with transmission function of $O(x, y)$, and the diffraction pattern intensity $I(u, v)$ is recorded using a charge-coupled device (CCD) camera in the far field of the specimen.

To simplify the reconstruction process, an aperture $A(x_0, y_0)$ connecting the screen smaller than $T(x_0, y_0)$
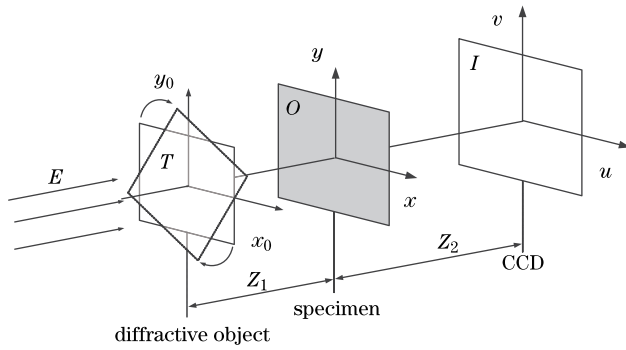
Fig. 1. Optical setup used for diffraction pattern recording.

is used to reduce the illumination area of the plane wave with amplitude E. In addition, the aperture synchronously rotates with the diffractive object. Considering that the plane wave transmits along the optic axis and the modulus and phase of the plane wave are constants, the screen exit wave with different rotation angle can be briefly described by rotating the screen exit wave $E \cdot A(x_0, y_0) \cdot T(x_0, y_0)$ with the same angle and the illumination on specimen can be rotated in the same way.

The illumination of the object studied without rotation can be described by $B(x, y) = \Im[E \cdot A(x_0, y_0) \cdot T(x_0, y_0), z_1]$, where $\Im$ presents the wave propagation with different distances. When the screen is rotated by angle $n\Delta\theta$, the illumination $P_n(x, y)$ on the specimen can be obtained by numerically rotating $B(x, y)$ by an angle of $n\Delta\theta$. This method can be described by $P_n(x, y) = R_n[B(x, y)]$, where R_n indicates the rotation operation with angle $n\Delta\theta$, and the subscript n indicates the distribution or process corresponding to the rotated angle $n\Delta\theta$. The exiting wave of the specimen without screen rotation is approximately described by $B(x, y) \cdot O(x, y)$. The light field on the CCD plane can be written as

$$\Psi(u, v) = \Im[B(x, y) \cdot O(x, y), z_2], \tag{1}$$

where z_2 is the distance between specimen and CCD, and $\Im$ indicates the forward Fresnel propagation. The intensity recorded by the CCD camera is $I_n(u, v) = |\Psi_n(u, v)|^2$.

In the data-recording procedure, when the screen is rotated by angle $n\Delta\theta$ ($n = 1 \cdots N$), the corresponding diffraction patterns I_n ($n = 1 \cdots N$) are recorded by the CCD camera in Fig. 1. Considering that the illumination on the specimen is unknown in most experiments (especially in this scheme), the ePIE algorithm is employed into the reconstruction process. Reconstruction operation is illustrated in Fig. 2. The iterative procedure between specimen plane (x, y) and CCD plane (u, v) starts with two random guesses $B_1(x, y)$ and $O_1(x, y)$. The subscript n of $P_n(x, y)$ represents $B(x, y)$ rotation with $n\Delta\theta$ angle, whereas the subscript n of other parameters present the initial nth estimation in the iteration. The nth iteration of a single circulation is described as follows.

1) The illumination estimate $P_n(x, y)$ of the specimen is calculated by numerically rotating $B_n(x, y)$ with an angle of $n\Delta\theta$ by $P_n(x, y) = R_n[B_n(x, y)]$. The guessed complex

amplitude distribution $\Psi_n(u, v)$ in the CCD plane is

$$\Psi_n(u, v) = \Im[P_n(x, y) \cdot O_n(x, y), z_2] = |\Psi_n(u, v)|e^{i\theta_n(u,v)}, \tag{2}$$

where $|\Psi_n(u, v)|$ and $\theta_n(u, v)$ are the amplitude and phase of $\Psi_n(u, v)$, respectively.

2) The magnitude constraint is applied by keeping the $\Psi_n(u, v)$ phase unchanged and replacing its modulus with the square root of the recorded I_n.

$$\Psi_n(u, v) = \sqrt{I_n}e^{i\theta_n(u,v)}. \tag{3}$$

3) $\Psi_n(u, v)$ is inversely propagated to the specimen plane to obtain an improved estimation of specimen exiting wave function using

$$\Phi_n(x, y) = \Im^{-1}[\Psi_n(u, v), z_2], \tag{4}$$

where $\Im^{-1}[\Psi_n(u, v), z_2]$ represents the backward Fresnel propagation of wave function $\Psi_n(u, v)$ for the distance z_2.

4) Specimen transmission function and illumination is updated according to[10]

$$O_{n+1}(x, y) = O_n(x, y) + \frac{|P_n(x, y)|}{|P_n(x, y)|_{\max}} \frac{P_n^*(x, y)}{[|P_n(x, y)|^2 + \alpha]}$$
$$\cdot [\Phi_n(x, y) - P_n(x, y) \cdot O_n(x, y)], \tag{5}$$

$$B_{n+1}(x, y) = B_n(x, y)$$
$$+ R_{-n}\left\{ \frac{|O_n(x, y)|}{|O_n(x, y)|_{\max}} \frac{O_n^*(x, y)}{[|O_n(x, y)|^2 + \alpha]} \right.$$
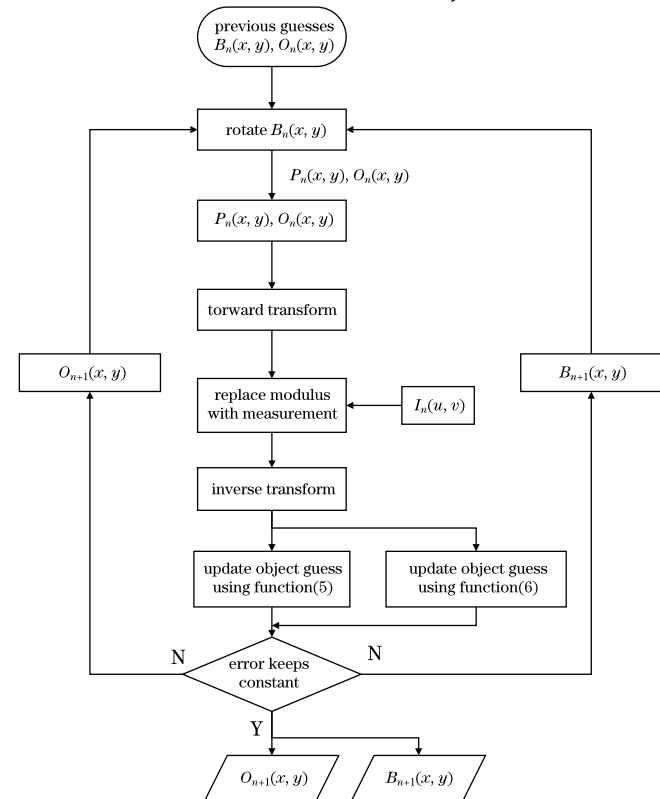$$\left. \cdot [\Phi_n(x, y) - P_n(x, y) \cdot O_n(x, y)] \right\}, \tag{6}$$

Fig. 2. Flowchart of the method with rotating illumination.

where R_{-n} (i.e., the rotation operation with angle $-n\Delta\theta$) presents the inverse progress of R_n, α is a constant parameter that avoids a zero value of $|O_n(x,y)|^2$, $|O_n(x,y)|_{\max}$ is the maximum value of the $O_n(x,y)$ amplitude, and the superscript * signifies conjugate.

5) $O_{n+1}(x,y)$ and $B_{n+1}(x,y)$ are used as the new guesses for the next iteration.

6) Steps 1 to 5 are repeated until the error is sufficiently small or remain unchanged between two successive iterations. The error is calculated according to

$$E_{\text{error}} = \frac{\sum |O_n(x,y) - O(x,y)|^2}{\sum |O(x,y)|^2}, \qquad (7)$$

where $O_n(x,y)$ is the reconstructed version of specimen transmission function, and $O(x,y)$ is the original transmission function of specimen.

7) If needed, the screen exit wave can be obtained by inversely propagating $B_n(x,y)$ to the screen plane, and the screen exit wave can represent the modulus and phase distribution of the screen because the incident illumination is plane wave.

To illustrate the feasibility of the algorithm proposed above, a numerical simulation is performed using the setup in Fig. 1. The modulus and phase of transmission function of the specimen used for calculation are shown in Figs. 3(a) and (b), respectively. A 632-nm uniform planar wave is used to illuminate the screen adjacent to a square aperture. In addition, the corresponding modulus and phase of the screen are given in Figs. 3(c) and (d), respectively. The CCD is assumed to have 1024×1024 pixels, and each pixel has the size of 7.4×7.4 (μm). The distance between the specimen and screen, as well as the distance between the CCD camera and specimen, are both 150 mm. Thirty-six frames of diffraction patterns $I_n(n = 1, 2, 3\cdots)$ are calculated according to Fresnel diffraction theory, and the corresponding rotation angle is $n\Delta\theta$, where $\Delta\theta = 10°$.

Given that various kinds of noises such as dark current noise are unavoidable in many experiments, Poisson noise similar to that in Fig. 4(a) is added to all the
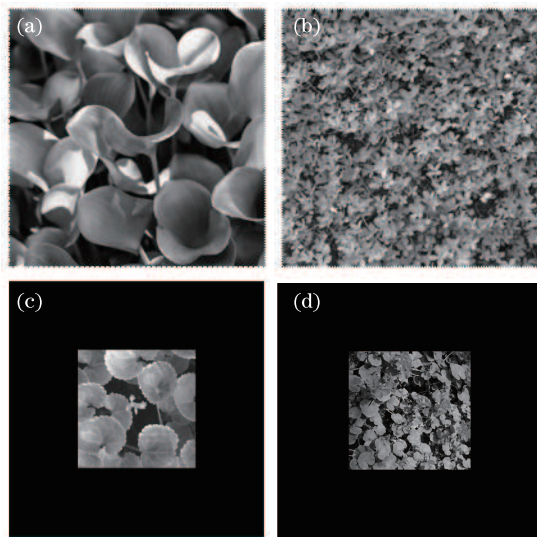

Fig. 3. Original specimen of simulation with (a) amplitude and (b) phase, and (c) the amplitude and (d) phase of the original screen adjacent to a square aperture.
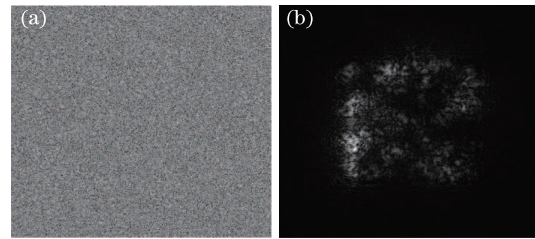

Fig. 4. (a) Random noise added into diffraction pattern; (b) the diffraction pattern intensity with random noise.
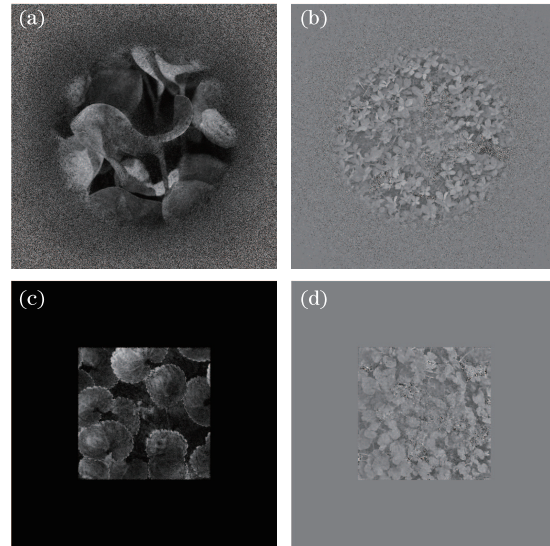

Fig. 5. Reconstructed images of specimen with suggested rotating illumination method. (a) Amplitude of specimen, (b) phase of specimen, (c) amplitude of screen, and (d) phase of screen.

calculated diffraction patterns. Figure 4(b) shows one of the diffraction patterns. Using the algorithm above, both the screen and the specimen can be reconstructed simultaneously. The reconstructions after 720 iterations are shown in Fig. 5. By comparing the reconstruction to the original images in Fig. 3, the quality of the reconstructed specimen image is found to be satisfying.

For comparison, another simulation with common $x-y$ scanning ePIE algorithm is also performed with Fig. 1. Considering practical situation, 1 pixel hysteresis error is added to the simulation process. To obtain approximately 50% overlapping for two neighboring positions, the screen is shrinked to one fourth of its original size. In addition, the result of 720 iterations is shown in Fig. 6, where obvious noise can be found, compared with Fig. 5. The center of the reconstructed amplitudes is selected to calculate peak signal-to-noise ratio (PSNR) for quantitative comparison according to

$$\text{PNSR} = 10 \times \lg\left[\frac{(2^n - 1)^2}{\text{MSE}}\right], \qquad (8)$$

where MSE is the mean squared error between reconstructed amplitudes. The PSNR of Fig. 5(a) is 73.57 dB, whereas the PSNR of Fig. 6(a) is 69.52 dB.

A difference is noted between Figs. 5 and 6 because using the rotating illumination method, the sample
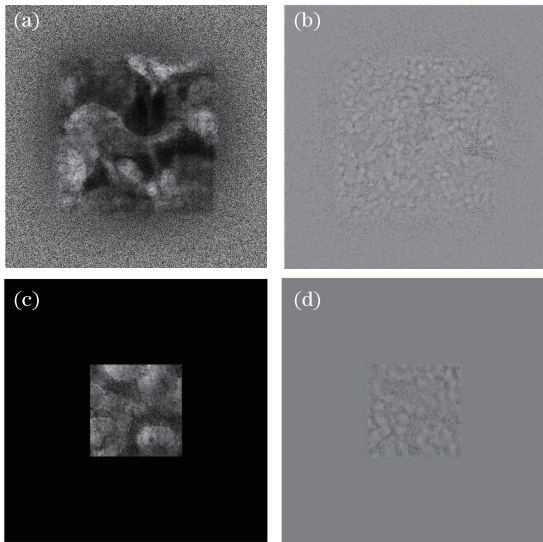
Fig. 6. Reconstructed images of specimen with $x - y$ scanning ePIE algorithm. (a) Amplitude of specimen, (b) phase of specimen, (c) amplitude of screen, and (d) phase of screen.
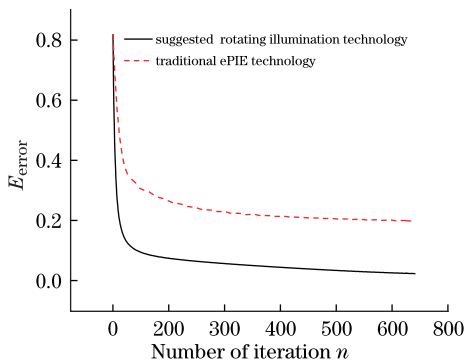

Fig. 7. Errors of the suggested rotating illumination method and standard ePIE algorithm with varying iterations.

function is updated 720 times in the whole image field. However, for the $x-y$ scanning method, the sample function is essentially updated for approximately 20 times (720/36=20).

For quantitative evaluation, the reconstruction error changes with the current iteration (Fig. 7), where the solid line indicates the reconstruction error of the suggested rotating illumination method, and the dashed line indicates the reconstruction error of the common $x - y$ scanning ePIE algorithm. The error is calculated according to Eq. (7).

For both algorithms, the reconstructed error becomes lower than 25% after 720 iterations. This error can be reduced further with more iterations. For practical experiments, the suggested rotating illumination method presents no backlash error; therefore, this method should

generate more accurate reconstruction. This result well-matches our theoretical results.

In conclusion, a rotating illumination algorithm is proposed to retrieve the transmission function of a specimen. In rotating illumination algorithm, the plane wave transmitting a rotatable screen is used as illumination on the specimen. The exit wave of the screen and the specimen can be reconstructed simultaneously with a modified ePIE algorithm. In the proposed method, the scanning motion that is needed in conventional ePIE is replaced by rotating the screen; notably, the rotation accuracy should be carefully observed. Since the screen always rotates in the given direction, the backlash error and the hysteresis of the stage, which are two of the main disadvantages of standard PIE method, need not be considered anymore. Furthermore, the proposed method can be used in limited space where scanning motion is not available. Thus, the feasibility of PIE algorithm is improved for many applications.

References

1. R. W. Gerchberg, Optik **35,** 237 (1972).
2. J. R. Fienup, Opt. Lett. **3,** 27 (1978).
3. J. R. Fienup, Appl. Opt. **21,** 2758 (1982).
4. C. Liu, T. Walther, and J. M. Rodenburg, Ultramicroscopy **109,** 1263 (2009).
5. K. P. Köstli and Beard, Appl. Opt. **42,** 1899 (2003).
6. J. R. Fienup, Appl. Opt. **32,** 1737 (1993).
7. W. Chen, G. Situ, and X. Chen. Opt. Express **21,** 24680 (2013).
8. F. Zhang, G. Pedrini, and W. Osten, Phys. Rev. A **75,** 043805 (2007).
9. W. Chen and X. Chen, Opt. Express **18,** 13536 (2010).
10. J. M. Rodenburg and H. M. L. Faulkner, Appl. Phys. Lett. **85,** 4795 (2004).
11. H. M. L. Faulkner and J. M. Rodenburg, Phys. Rev. Lett. **93,** 023903 (2004).
12. J. M. Rodenburg, A. C. Hurst, A. G. Cullis, B. R. Dobson, F. Pfeiffer, O. Bunk, C. David, K. Jefimovs, and I. Johnson, Phys. Rev. Lett. **98,** 034801 (2007).
13. X. Pan, S. P. Veetil, C. Liu, Q. Lin, and J. Zhu, Chin. Opt. Lett. **11,** 021103 (2013).
14. A. M. Maiden and J. M. Rodenburg, Ultramicroscopy **109,** 1256 (2009).
15. A. M. Maiden, M. J. Humphry, M. C. Sarahan, B. Kraus, and J. M. Rodenburg, Ultramicroscopy **120,** 64 (2012).
16. F. Liu, Z. Liu, L. Zheng, H. Huang, and J. Zhu, High Power Laser Sci. Eng. **1,** 29 (2013).